Chinese J. Chem. Eng., **11** (6) 638 – 642 (2003)

Influence of Feed Injection on Hydrodynamic Behavior in FCC Riser*

SUN Guogang(孙国刚) ** **and SHI Mingxian(时铭显)**
Department of Chemical Engineering, University of Petroleum, Beijing 102249, China

Abstract This paper studies the influence of feed injection on the hydrodynamic behavior of fluid catalytic cracking riser reactors. Experiments were conducted in a cold model of 186 mm ID with two oppositely inclined secondary air feed nozzles. The flow structure was determined by means of the axial static pressure measurements and local radial optic fiber probe measurements on different levels with emphasis on the sections downstream of the secondary injection. The measurements reveal that the secondary injection plays a crucial role on riser hydrodynamics. Just above the secondary injection, the flow and mixing are strongly affected, while below the secondary injection the effect is weak. The radial profile just downstream of secondary injection demonstrates wavy features. The effective region of secondary injection could be estimated by the axial pressure gradient profiles and/or the radial profiles of local solids velocity and density.
Keywords fluid catalytic cracking, riser reactor, feed injection region, flow structure

1 INTRODUCTION

Most commercial circulating fluidized bed(CFB) risers involve the injection of one or more gas streams along the riser. For example, in CFB boilers, secondary air is supplied in staged combustion for reducing NO_x emission and controlling temperature of the dense phase. In fluid catalytic cracking (FCC) units, atomized oil droplet streams are injected through several inclined feed nozzles to promote fast mixing and intimate contact between the oil and catalysts for increasing conversion and selectivity. In spite of wide utilization of secondary gas injection, research on the influence of secondary gas injection on riser hydrodynamics is scarcely reported.

Recently some papers dealing with the effects of secondary gas injection on the gas and solids flow patterns in CFB risers were published. Wang and Gibbs[1] studied the variation of pressure drop, which is assumed to be proportional to solids concentration, both in the regions above and below the secondary gas port with radial or swirling injections. Arena *et al.*[2], Marzocchella and Arena [3] measured the mixing phenomena between the rising gas-solids suspension and the lateral gas stream from a slot over the whole circumference of the riser or four equally spaced radial jets in the riser. Cho *et al.*[4] examined the variation of axial solids hold up with a tangential or a radial secondary injection. Aguillon *et al.*[5] measured the local solids flux and velocity in a rectangular riser with different air injection levels. Zijlma *et al.*[6] studied the influence of co-current or counter-current air injection on both solids distribution and circulation rate in the riser. However, all the secondary gas injection configurations examined do not resemble the FCC feed-injection system in which the oil feed nozzles inclined to the riser axis ranging from 30° to 60° are commonly mounted. Furthermore, operations of the above apparatus, except for the experiments of Arena *et al.*[2] (with $U_g = 15\,m{\cdot}s^{-1}$ and $G_s = 210\,kg{\cdot}m^{-2}{\cdot}s^{-1}$), were also at lower solids circulation flux ($< 60\,kg{\cdot}m^{-2}{\cdot}s^{-1}$), more close to the operating conditions of a CFB boiler rather than a FCC unit.

For understanding the phenomena involved in the feed injection zone of a FCC riser reactor and further for the FCC process optimization, a series of numerical simulation and experimental studies[7–11] have been conducted recently in the University of Petroleum, Beijing. In this paper, the effect of secondary air injection by two upward inclined nozzles on the hydrodynamic behavior of a cold FCC riser is presented. Attention is focused on variation in radial profiles of the solid phase downstream of secondary air injection.

2 EXPERIMENTAL

The experimental apparatus is shown in Fig. 1. It has been described in detail elsewhere (Sun *et al.*[12]). The riser consists of a 186 mm ID, 14 m high plexiglass pipe, equipped with 28 taps for pressure transducers. Carrier gas is atmospheric air, supplied by a Roots blower, and flowrates are measured with several standard rotameters. FCC catalyst used in the study has a mean volumetric diameter of 56 μm and a bulk density of $850\,kg{\cdot}m^{-3}$. Its minimum fluidization velocity is $0.003m{\cdot}s^{-1}$. The solids re-circulation down-

Received 2003-04-30, accepted 2003-08-22.
* Supported by the National Natural Science Foundation of China (No. 29976024).
** To whom correspondence should be addressed. E-mail: ggsun@163bj.com

comer of 300 mm diameter is equipped with a sieve-plate butterfly valve covered by wire mesh installed in the upper downcomer for measurement of the solids flux. The solids flux is calculated by measuring the time for a known volume of solids to accumulate on top of the butterfly valve after it is closed. The gas-solids suspension density in the riser is assumed to be inferred from the measurements of pressure drop along the riser.

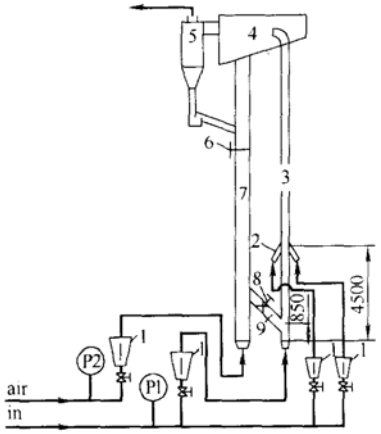

Figure 1 Schematic diagram of experimental apparatus

1—flowmeter; 2—secondary air nozzle; 3—riser; 4—disengagement chamber; 5—cyclone; 6—measuring butterfly valve; 7—downcomer; 8—butterfly valve; 9—inclined pipe

Figure 2 illustrates the configuration of the two opposed secondary air feed nozzles. The nozzle outlet is a rectangle of 40 mm×10 mm. Local averaged suspension density at different radial positions inside the riser is measured by an optical fiber probe and local solids velocity measurement is carried out with a double fiber probe based on cross-correlation of the two probe signals. The optic fiber probe measurements are performed in three radial directions with $\beta = 0°$, 45° and 90° as shown in Fig. 2, in order to detect the flow asymmetry in the riser with secondary injection.

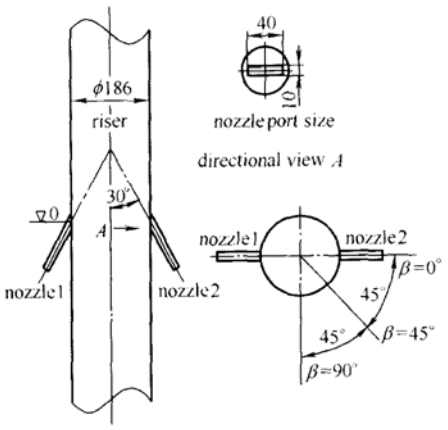

Figure 2 Secondary air feed injection system

3 RESULTS AND DISCUSSION

3.1 Axial pressure gradient profiles

Riser axial pressure profile, local solids velocity and suspension density were measured under several operating conditions such as with various gas feed rate at the riser bottom, solids circulation rate, and secondary air rate. Typical axial pressure gradient profiles with and without secondary air injection at constant solids circulation flux are given in Fig. 3, showing the macro-aspects of the influence of secondary gas injection on the riser hydrodynamics.

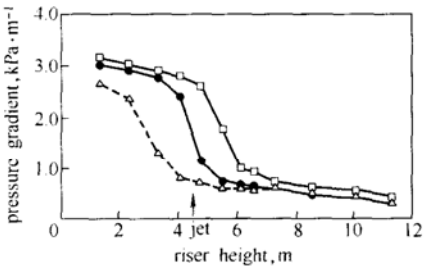

Figure 3 Typical pressure gradient profiles
($G_s = 160\,kg\cdot m^{-2}\cdot s^{-1}$)
$U_{p,l}$, $m\cdot s^{-1}$: □ 2.25; ● 2.25; △ 3.48
U_j, $m\cdot s^{-1}$: □ 0; ● 41.7; △ 0
U_g, $m\cdot s^{-1}$: □ 2.25; ● 3.48; △ 3.48

Since the secondary gas injection divides the riser into two zones of different superficial gas velocity, namely a primary zone below the injection port with gas velocity denoted as $U_{p,l}$ (preliminary lifting gas velocity) and a secondary zone above the injection port with gas velocity U_g. The pressure gradients at $U_{p,l} = U_g = 2.25\,m\cdot s^{-1}$ and $3.48\,m\cdot s^{-1}$ without secondary injections are also plotted in Fig. 3 for comparison. From Fig. 3, at least four features can be seen. First, at the same preliminary lifting gas velocity ($U_{p,l} = 2.25\,m\cdot s^{-1}$), secondary air injection reduces the riser axial pressure drop, indicating a lower riser suspension density at that point. Great differences mainly exist in the axial pressure gradient profiles downstream of the injection. This demonstrates that the influence of secondary gas injection on the riser flow is significant in the upper part just above the injection and marginal below the injection. Second, for the same riser exit gas velocity ($U_g = 3.48\,m\cdot s^{-1}$), axial pressure drop is higher with secondary air injection. On the other hand, significant increase of axial pressure gradient is seen in the lower section of the riser, whereas the profile in the upper is almost identical. The secondary air injection is assumed to act as a barrier for upward solids flow. The lower primary lifting air velocity also has contributions to the higher solids density in the riser bottom. Third, only in a

specific region immediately below and above the injection port (effective region of secondary gas injection) the secondary gas injection does affect the riser flow behavior significantly. Outside this region, the influence of secondary injection might be negligible. And fourth, two distinctive regions are clearly recognizable in axial pressure gradient profiles, whether secondary air is injected or not. All axial profiles in Fig. 3 are S-shape. This implies that the riser axial profile with secondary gas injection might be predicted by modifying the CFB models, such as the model of Li and Kwauk[13].

3.2 Radial profiles of axial solids velocity and suspension density

Figure 4 shows the radial profiles of local solids axial velocity in the downstream of the secondary injection. The measurements are performed at $U_{p,l} = 3.28\,m\cdot s^{-1}$ and secondary air injection velocity $U_j = 41.7\,m\cdot s^{-1}$. The flow rate ratio of secondary air to total air in the riser is 27.3%, resulting in $U_g = 4.5\,m\cdot s^{-1}$ and corresponding solid flux $G_s = 230\,kg\cdot m^{-2}\cdot s^{-1}$ downstream of the injection. The difference of the solids fluxes calculated by integrating the radial profiles of solids axial velocity and suspension density and by the sieve-plate butterfly valve is below 20%. The secondary air injection port is 4.5 m above the riser bottom gas distributor. Fig. 5 illustrates the suspension density radial profiles in the same operation condition as Fig. 4. From Figs. 4 and 5, intense asymmetry and non-uniformity in radial profiles are found in the zones immediately above injection. The radial profile shapes of the solids velocity and suspension density for the three radial orientations ($\beta = 0°$, 45°, 90°) are quite different. These indicate that there exists a complex interaction between the secondary injection stream and gas-solids suspension rising from the riser bottom.

Dramatic variations in the radial profiles of solids velocity and density are observed in the sections downstream of the secondary injection. At 0.19 m above the injection port (Fig. 4), the solids velocity radial profile becomes wavelike with three wavecrests in the $\beta = 0°$ direction. The amplitude of the wavy velocity profile increases in the section up to 0.375 m, and then is weakened at 0.675 m above the injection port. At $H = 1.4$ m above injection, the asymmetry in solids velocity radial profiles eventually vanishes. As expected, in Fig. 4 solids velocities increase significantly in the sections downstream of the injection. The same trend is evident in Fig. 5. The suspension density profiles display strong wavy feature at 0.19 m. The wavy feature decays at 0.375 m. The comparison of Fig. 4 with Fig. 5 reveals that the wavy profile of suspension density appears earlier than that of solids velocity. A

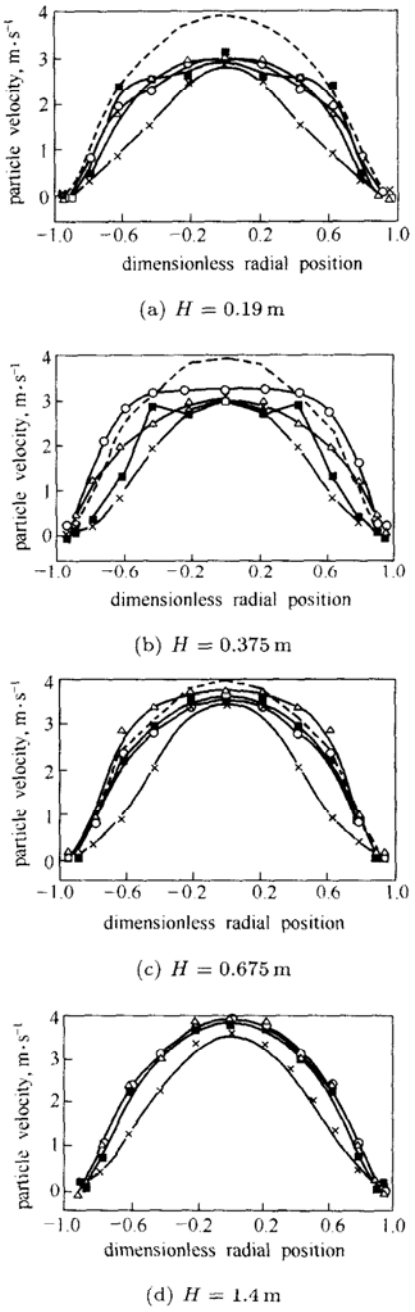

Figure 4 Radial profiles of solids axial velocity downstream of secondary injection
($U_{p,l} = 3.28\,m\cdot s^{-1}$, $U_j = 41.7\,m\cdot s^{-1}$, $U_g = 4.5\,m\cdot s^{-1}$, $G_s = 230\,kg\cdot m^{-2}\cdot s^{-1}$)
β: ■ 0°; ○ 45°; △ 90°
solid velocity without secondary injection:
× $U_g = U_{p,l} = 3.28\,m\cdot s^{-1}$; - - - - $U_g = 4.5\,m\cdot s^{-1}$

higher suspension density zone is clearly observed at the riser center at 0.19 m and 0.375 m (Fig. 5). These phenomena suggest that the two secondary air streams do not impinge on each other and do not reach the center of riser. The effects of the injection decays gradually with the distance increased from the injection port. Approaching the 0.675 m section, the wavy feature in the profiles disappears, though there is

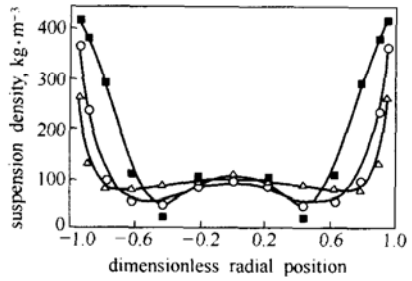

(a) $H = 0.19$ m

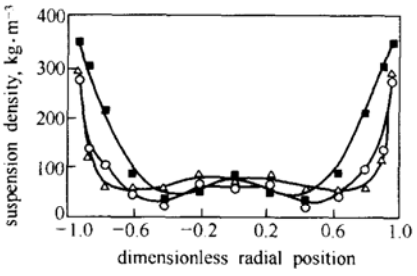

(b) $H = 0.375$ m

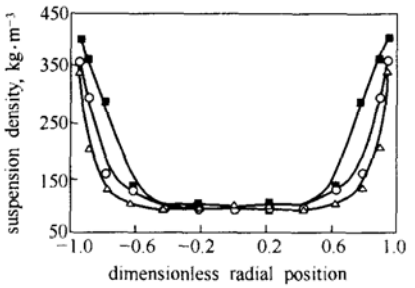

(c) $H = 0.675$ m

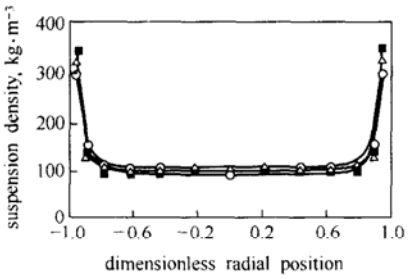

(d) $H = 1.4$ m

Figure 5 Radial profiles of suspension density downstream of secondary injection
($U_{p,l} = 3.28\ m\cdot s^{-1}$, $U_j = 41.7\ m\cdot s^{-1}$, $U_g = 4.5\ m\cdot s^{-1}$, $G_s = 230\ kg\cdot m^{-2}\cdot s^{-1}$)
β: ■ 0°; ○ 45°; △ 90°

still substantial difference among the suspension density profiles of the three measured directions. Coinciding with the solids velocity profiles, at 1.4 m above the secondary injection port, the radial profiles of suspension density evolve into typical symmetric core-annulus structure as usually observed in risers without secondary injection. These indicate that the interaction between secondary air stream and gas-solids suspension is complete and the effect of secondary injection vanishes at this 1.4 m downstream level, which agrees roughly with that obtained from pressure measurements.

At the section of 0.2 m below the secondary injection, the solids velocity radial profiles (Fig. 6) change very little for the three measured directions. A symmetric core-annular flow structure is still preserved. The solids velocity increases a little, compared with the same $U_{p,l}$ riser operation without secondary injection. The solids velocity profiles with and without secondary injection are quite similar. A nearly identical situation is also observed in suspension density radial profiles(Fig. 7).

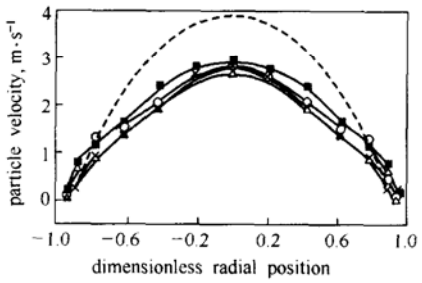

Figure 6 Solids velocity radial profiles below secondary injection
($H = -0.2$ m, $U_{p,l} = 3.28 m\cdot s^{-1}$, $U_j = 41.7\ m\cdot s^{-1}$, $U_g = 4.5\ m\cdot s^{-1}$, $G_s = 230\ kg\cdot m^{-2}\cdot s^{-1}$)
β: ■ 0°; ○ 45°; △ 90°
solid velocity without secondary injection:
× $U_g = U_{p,l} = 3.28\ m\cdot s^{-1}$; - - - - - $U_g = 4.5\ m\cdot s^{-1}$

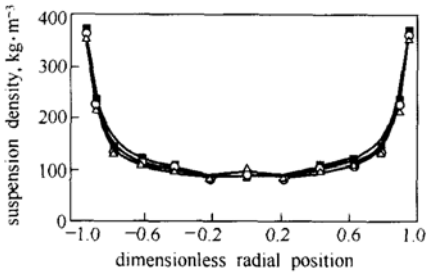

Figure 7 Suspension density profiles below secondary injection
($H = -0.2$ m, $U_{p,l} = 3.28\ m\cdot s^{-1}$, $U_j = 41.7\ m\cdot s^{-1}$, $U_g = 4.5\ m\cdot s^{-1}$, G_s=230 $kg\cdot m^{-2}\cdot s^{-1}$)
β: ■ 0°; ○ 45°; △ 90°

With secondary injection, only a small decrease in the riser density is seen. These observations suggest that the influence of secondary injection on the upstream section is weak.

4 CONCLUSIONS

The influence of secondary air feed injection on a cold FCC riser was experimentally examined. The measurements have improved the understanding of the hydrodynamic flow behavior in the FCC feed injection zone. The following conclusions can be drawn:

(1) For the same preliminary lifting gas velocity, secondary gas feed injection affects strongly the hydrodynamics of the upper part above the injection level, while its effect is nearly negligible below the injection level.

(2) The radial profiles of local solids velocity and suspension density both display wavy features in the region just downstream secondary air injection, indicating complex interaction or mixing between the secondary streams and gas-solids suspension rising from the riser bottom.

(3) The effective region of secondary injection can be estimated from the axial pressure gradient profile and/or the radial profiles of local solids velocity and suspension density.

(4) Predicting the axial pressure gradient profiles of the riser with secondary air injection is possible.

Data presented in this paper include only the results obtained with constant preliminary lifting gas velocity $U_{p,l}$, secondary gas injection velocity U_j and solids circulation rate G_s. Other results obtained at various $U_{p,l}$, U_j and G_s will be reported later.

NOMENCLATURE

G_s	solids-circulating rate, $kg \cdot m^{-2} \cdot s^{-1}$
H	height level from secondary injection port, m
U_g	superficial gas velocity above secondary injection port, $m \cdot s^{-1}$
U_j	secondary gas injection velocity, $m \cdot s^{-1}$
U_p	local solid velocity, $m \cdot s^{-1}$
$U_{p,l}$	preliminary lifting superficial gas velocity below secondary injection port, $m \cdot s^{-1}$
β	radial orientation, (°)
ρ_s	local suspension density, $kg \cdot m^{-3}$

REFERENCES

1 Wang, X.S., Gibbs, B.M., "Hydrodynamics of a circulating fluidized bed with secondary air injection", In: Circulating Fluidized Bed Technology Ⅲ, Basu, P., Horio, M., Hasatani, M., Eds., Pergamon Press, Oxford, 225—230 (1991).

2 Arena, U., Marzocchella, A., Bruzzi, V., Massimilla, L., "Mixing between a gas-solid suspension flowing in a riser and a lateral gas stream", In: Circulating Fluidized Bed Technology Ⅳ, Avidan, A., Ed., AIChE , New York, 545—550 (1993).

3 Marzocchella, A., Arena, U., "Hydrodynamics of a circulating fluidized bed operated with different secondary air injection devices", *Powder Technol.*, **87**, 185—191 (1996).

4 Cho, Y.J., Namkung, W., Kim, S.D., Park, S., "Effect of secondary air injection on axial solid holdup distribution in a circulating fluidized bed", *J. Chem. Eng. Japan*, **27** (2), 158—164 (1994).

5 Aguillon, J., Shakourzadeh, K., Guigon, P., Large, J.F., "Hydrodynamic behaviour of circulating fluidized bed with secondary air injection", In:Circulating Fluidized Bed Technology V, Beijing, DGS4 (1996).

6 Zijlma, G.J., Gerritsen, A.W., Van Bleek, C.M., "Influence of secondary air injection on solids distribution and circulation rate in a CFB", In:Circulating Fluidized Bed Technology Ⅵ, Werther, J., Ed., DECHEMA e.V., 27—32 (1999).

7 Gao, J.S., Xu, C.M., Yang, G.H., Guo, Y.C., Lin, W.Y., "Numerical simulation on gas-solid two-phase turbulent flow in FCC riser reactors (I): Turbulent gas-solid flow reaction model", *Chinese J. Chem. Eng.*, **6** (1), 12—20 (1998).

8 Gao, J.S., Xu, C.M., Lin, S.X., Guo, Y.C., Wang, X.L., "Numerical simulation on gas-solid two-phase turbulent flow in FCC riser reactors (Ⅱ): Numerical simulation on the gas-solid two-phase turbulent flow", *Chinese J. Chem. Eng.*, **6** (1), 21—28 (1998).

9 Gao, J.S., "Numerical simulation on the flow, heat-transfer and reaction in the catalytic cracking riser reactors", Ph. D. Thesis, University of Petroleum, Beijing (1997). (in Chinese)

10 Fan, Y.P., "Gas-solid two-phase flow in FCC riser", Ph. D. Thesis, University of Petroleum, Beijing (2000). (in Chinese)

11 Fan, Y.P., Ye, S., Lu, C.X., Sun, G., G., Shi, M.X., "Gas-solid two-phase flow in FCC riser", *AIChE J.*, **48** (9), 1869—1887 (2002).

12 Sun, G.G., Chao, Z.X., Fan, Y.P., Shi, M.X., "Hydrodynamic behavior in the bottom region of a cold FCC riser", In: Circulating Fluidized Bed Technology Ⅵ, Werther, J., Ed, DECHEMA e.V., 179—184 (1999).

13 Li, Y., Kwauk, M., "The dynamics of fast fluidization", In: Fluidization, Grace, J. R., Matsen, J. M., Eds., Plenum Press, Oxford, 537—544 (1980).